Received: March 10, 2015 | Accepted: April 3, 2015 | Web Released: April 9, 2015 CL-150213

Synthesis, Structural Characterization, and Oxidation Catalysis of a Diniobium-substituted Silicodecatungstate

Naoto Satake, Tomohisa Hirano, Keigo Kamata,† Kosuke Suzuki, Kazuya Yamaguchi, and Noritaka Mizuno*
Department of Applied Chemistry, School of Engineering, The University of Tokyo, 7-3-1 Hongo, Bunkyo-ku, Tokyo 113-8656

(E-mail: tmizuno@mail.ecc.u-tokyo.ac.jp)

A novel diniobium-substituted silicodecatungstate, [γ-$HSiW_{10}O_{38}Nb_2(\eta^2\text{-}O_2)_2]^{5-}$ (**I**), was successfully synthesized by the reaction of $[HNb_6O_{19}]^{7-}$ and [γ-$SiW_{10}O_{36}]^{8-}$ in the presence of H_2O_2 under acidic conditions. In the presence of a suitable proton source, e.g., $HClO_4$, **I** could act as a stable homogeneous catalyst for H_2O_2-based oxidation.

Polyoxometalates (POMs) are early transition-metal (V, Nb, Ta, Mo, W, etc.) oxygen cluster anions with discrete and versatile structures and have attracted much attention in various fields of science such as catalysis, medicine, and advanced material science.[1] In particular, POMs are promising oxidation catalysts owing to the following advantages: (i) Catalytically active sites can precisely be created at atomic and/or molecular levels and (ii) they are relatively stable under thermal and oxidative conditions.[2] Hydrogen peroxide (H_2O_2) is an ideal oxidant because of its high content of active oxygen species and coproduction of only water. Therefore, a large number of H_2O_2-based oxidation systems with POM-based catalysts such as peroxometalates, lacunary POMs, and transition-metal-substituted POMs have been developed to date.[3]

It is known that d^0-transition-metal-substituted POMs can efficiently catalyze the H_2O_2-based oxidation of various kinds of organic substrates.[4,5] In particular, the activation of H_2O_2 by titanium-[4] and vanadium-substituted POMs,[5] and their oxidation catalysis have extensively been investigated. On the other hand, there are only a few reports on H_2O_2-based oxidation catalysis by niobium-substituted POMs.[6] While allylic alcohols are selectively oxidized to the corresponding triols with H_2O_2 in the presence of triniobium-substituted POMs such as $[H_2Si_2W_{18}Nb_6O_{77}]^{6-}$ and A,β-$[PW_9O_{37}(NbO_2)_3]^{6-}$, these POMs are not active for the epoxidation of simple alkenes.[6] In addition, these POMs are decomposed into peroxotungstate fragments to some extent because of the presence of excess amounts of H_2O_2, which are the truly catalytically active species for the oxidation of allylic alcohols.[6] Therefore, successful examples of POMs with well-defined niobium centers, which can activate H_2O_2 and catalyze the oxidation of various substrates, including simple alkenes, have not yet been reported.

Herein, we report the successful synthesis and structural characterization of a novel diniobium-substituted silicodecatungstate, [γ-$HSiW_{10}O_{38}Nb_2(\eta^2\text{-}O_2)_2]^{5-}$ (**I**). In the presence of a suitable proton source, e.g., $HClO_4$, **I** could act as a stable homogeneous catalyst for the H_2O_2-based oxidation of several organic substrates, e.g., cyclooctene, thioanisole, 1-phenylethanol, and allyl alcohol. The reaction mechanism, including the effect of protons on the formation of active species, was also investigated.

The tetra-*n*-butylammonium (TBA) and tetra-*n*-pentylammonium (TPeA) salts of **I** (TBA_5**I** and $TPeA_5$**I**, respectively) were synthesized by the reaction of $K_7[HNb_6O_{19}]\cdot 13H_2O$, K_8[γ-$SiW_{10}O_{36}]\cdot 12H_2O$, and the corresponding alkylammonium bromide in the presence of H_2O_2 under acidic conditions (see the Supporting Information). The tetramethylammonium (TMA) salt of **I** (TMA_5**I**) was also synthesized by the cation-exchange reaction of TBA_5**I** with $TMANO_3$. The IR spectra of TMA_5**I**, TBA_5**I**, and $TPeA_5$**I** showed bands around 830, 600, and 550 cm^{-1} assignable to υ(O–O), υ_{asym}(Nb(O_2)), and υ_{sym}(Nb(O_2)), respectively, and these band positions are close to those of typical peroxoniobates (Figure S1).[6–8]

Single crystals of TMA_5**I** suitable for X-ray crystallographic analysis were successfully obtained from a mixed solvent of acetonitrile and water containing crude TMA_5**I** with vapor diffusion of diethyl ether. The crystallographic data are summarized in Table S1, and the ORTEP representation of the anionic part of TMA_5**I** is shown in Figure 1. The anionic part of TMA_5**I** was a monomer of a diniobium-substituted γ-Keggin POM. One terminal η^2-peroxo group was coordinated to each of the two niobium atoms, and the O–O bond lengths (1.46–1.47 Å) were comparable to those of typical peroxoniobates (1.43–1.51 Å) (Table S2).[6–8] The elemental analysis and X-ray crystallographic analysis data revealed the existence of five TMA cations per anion. The bond valence sum (BVS) values of niobium (5.27–5.32), tungsten (6.04–6.20), and silicon (3.75) indicated that the respective valences were +5, +6, and +4. Therefore, one proton is probably associated with **I**. The BVS value of O38 (1.12) was significantly lower than those of other oxygen atoms (1.72–2.09), showing that O38 was possibly protonated. To the best of our knowledge, this is the first example of a structurally characterized diniobium-substituted γ-Keggin silicodecatungstate.

The positive-ion cold-spray ionization mass (CSI-MS) spectrum of TMA_5**I** in CD_3CN exhibited two sets of signals centered at *m*/*z* 3170 and 1622, with isotopic distributions

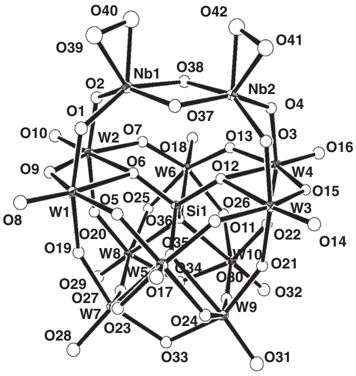

Figure 1. ORTEP drawing of the anion part of TMA_5**I** drawn at 50% probability level.

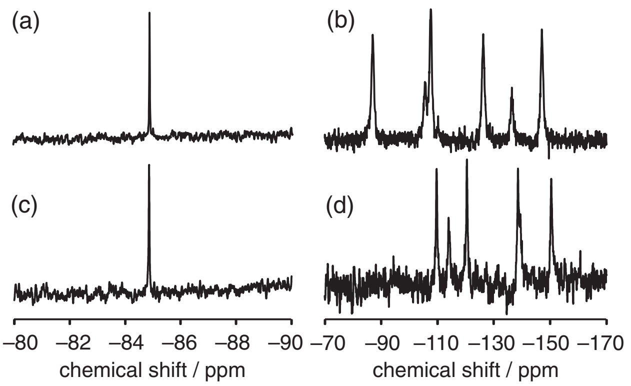

Figure 2. (a) ^{29}Si and (b) ^{183}W NMR spectra of TPeA$_5$**I**. (c) ^{29}Si and (d) ^{183}W NMR spectra of TPeA$_5$**I** in the presence of H_2O_2 and two equiv of $HClO_4$. Conditions for (a) and (c): TPeA$_5$**I** (0.03 M), 97% H_2O_2 (0 or 2.4 M), $HClO_4$ (0 or 0.06 M), CD_3CN, 233 K. Conditions for (b) and (d): TPeA$_5$**I** (0.1 M), 97% H_2O_2 (0 or 8.0 M), $HClO_4$ (0 or 0.2 M), CD_3CN, 233 K (see also Figure S3).

which agreed with the patterns calculated for $[TMA_6HSiW_{10}O_{38}Nb_2(O_2)_2]^+$ and $[TMA_7HSiW_{10}O_{38}Nb_2(O_2)_2]^{2+}$, respectively (Figure S2a). The CSI-MS spectra of TBA$_5$**I** and TPeA$_5$**I** showed similar intense signal sets (Figures S2b and S2c), suggesting that the solution states of **I** are the same regardless of the kind of cations. The ^{29}Si NMR spectrum showed one signal at −84.9 ppm (Figure 2a),[9] suggesting that TPeA$_5$**I** is a single species. The ^{183}W NMR spectrum showed six signals at −87.0, −105.6, −107.6, −126.2, −136.4, and −147.0 ppm with the respective intensity ratio of 2:1:2:2:1:2,[9] suggesting C_s symmetry in CD_3CN (Figure 2b). The stoichiometric oxidation of triphenylphosphine (1 mmol) with TPeA$_5$**I** (20 µmol) gave 39 µmol of triphenylphosphine oxide, showing that **I** has 2 equiv of active oxygen species for phosphine oxidation. All these CSI-MS and NMR results show that the solid-state structure of **I** is maintained in the solution state.

To confirm the catalytic activity of **I**, the TBA$_5$**I**-catalyzed epoxidation of cyclooctene (**1**) with H_2O_2 was carried out under various conditions (Table 1). In each case, 1,2-epoxycyclooctane (**2**) was mainly obtained with the formation of small amounts of the corresponding diol (**3**), hydroxy ketone (**4**), and enone (**5**). While TBA$_5$**I** itself showed low catalytic activity for the epoxidation, the reaction rates dramatically increased as the amounts of $HClO_4$ increased up to 2 equiv and did not change much upon addition of more than 2 equiv of $HClO_4$. The yield of **2** was also dependent on the amounts of $HClO_4$, and the yield of **2** reached up to 56% when using 2 equiv of $HClO_4$. The same dependence was also observed for the TPeA$_5$**I**-catalyzed epoxidation of **1** (Figure S4). In addition, the reaction rate for the catalytic epoxidation by TBA$_5$**I** with H_2O_2 in the presence of 2 equiv of $HClO_4$ (5.4×10^{-2} mM min^{-1}) was much larger than those for (i) the catalytic epoxidation by TBA$_5$**I** with H_2O_2 in the absence of $HClO_4$ (1.7×10^{-3} mM min^{-1}) and (ii) the stoichiometric epoxidation with TBA$_5$**I** in the presence of 2 equiv of $HClO_4$ (4.3×10^{-3} mM min^{-1}) (Figure S5). These results show that **I** requires both protons and H_2O_2 to achieve high catalytic performance, and that the further reaction of **I** with H_2O_2 likely proceeds in the presence of protons to give the active species for epoxidation.

Table 1. Effect of proton on the TBA$_5$**I**-catalyzed epoxidation of **1** with H_2O_2[a]

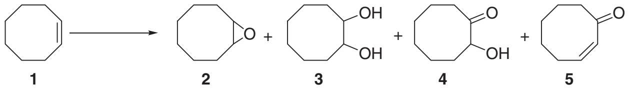

Entry	$HClO_4$/equiv	R_0 /mM min^{-1}	Yield/%	Selectivity to **2**/%
1	None	$(1.7 \pm 0.9) \times 10^{-3}$	9	>99
2	1	$(1.3 \pm 0.2) \times 10^{-2}$	48	98
3	2	$(5.4 \pm 0.7) \times 10^{-2}$	60	94
4	3	$(5.4 \pm 0.4) \times 10^{-2}$	67	91

[a] Reaction conditions: TBA$_5$**I** (4 µmol), **1** (1.0 mmol), 30% H_2O_2 (0.1 mmol), $HClO_4$ (0–3 equiv with respect to TBA$_5$**I**), CH_3CN (3 mL), 283 K, 24 h. Yield and selectivity were determined by GC analysis using chlorobenzene as the internal standard. Yield (%) = total products (mol)/initial H_2O_2 (mol) × 100. Selectivity (%) = desired product (mol)/total products (mol) × 100.

For early transition-metal complexes, protons play an important role in the formation of active species for epoxidation with H_2O_2.[10] In order to confirm the formation of the active species, the NMR (^{29}Si and ^{183}W) and CSI-MS spectra of TPeA$_5$**I** were measured in the presence of both H_2O_2 and protons (2 equiv of $HClO_4$).[9] The ^{29}Si NMR spectrum showed one signal at −84.9 ppm (Figure 2c), showing the formation of a single species. Upon addition of H_2O_2 and $HClO_4$, six signals appeared at −109.8, −114.0, −120.5, −138.6, −139.6, and −150.4 ppm with the respective intensity ratio of 2:1:2:2:1:2, and the chemical shifts were significantly different from those of **I** (Figure 2d). The 2:1:2:2:1:2 ratio suggested that the species also had C_s symmetry. The CSI-MS spectrum of TPeA$_5$**I** in the presence of H_2O_2 and 2 equiv of $HClO_4$ exhibited a set of intense signals centered at m/z 4400 assignable to a triperoxo species, $[\text{TPeA}_5\textbf{II}\cdot 2CH_3CN\cdot HClO_4]^+$ ($\textbf{II} = [SiW_{10}O_{36}Nb_2(O_2)_3]^{4-}$) (Figure S6a). Upon addition of **1** to the solution, the signals almost disappeared and new signals centered at m/z 4384 assignable to $[TPeA_5SiW_{10}O_{37}Nb_2(O_2)_2\cdot 2CH_3CN\cdot HClO_4]^+$ appeared (Figure S6b). These results show that **II** with C_s symmetry is the possible active species for epoxidation.

Kinetic studies on the epoxidation of **1** with H_2O_2 catalyzed by TBA$_5$**I** in the presence of 2 equiv of $HClO_4$ showed the first-order dependence of the reaction rates on the concentration of TBA$_5$**I** (0.67–2.67 mM, Figure S7a), while it has been reported that fractional order dependence is observed when using $[H_2Si_2W_{18}Nb_6O_{77}]^{6-}$ and A,β-$[PW_9O_{37}(NbO_2)_3]^{6-}$.[6] In addition, the NMR and CSI-MS signals assignable to peroxotungstate fragments were not observed during the catalytic reaction. These results indicate that **I** is stable under the reaction conditions.

In the case of divanadium-substituted POMs, $[\gamma\text{-}XW_{10}O_{38}V_2(\mu\text{-}OH)_2]^{n-}$ (X = Si ($n = 4$) or P ($n = 3$)), the reaction of the $\{V_2(\mu\text{-}OH)_2\}$ core with H_2O_2 gives the $\{V_2(\mu\text{-}OH)(\mu\text{-}OOH)\}$ species followed by successive dehydration to form an active oxygen species with the $\mu\text{-}\eta^2\text{:}\eta^2\text{-}O_2$ species.[5] Similarly, protons likely play an important role in the formation of the $\{Nb_2(\mu\text{-}OH)_2\}$ site, which would react with H_2O_2 to form the bridging peroxo species **II**, e.g. $\mu\text{-}\eta^2\text{:}\eta^2\text{-}O_2$, $\mu\text{-}\eta^1\text{:}\eta^1\text{-}O_2$ species.[11]

Finally, the scope of the present TBA$_5$**I**-catalyzed oxidation system was examined (Table 2). Cyclooctene selectively gave 1,2-epoxycyclooctane. The oxidation of thioanisole exclusively

Table 2. Oxidation of various substrates with H_2O_2 by TBA_5**I** in the presence of $HClO_4$[a]

Entry	Substrate	Time /h	Product (Selectivity/%)	Yield /%
1	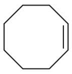	24	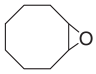 (94)	60
2	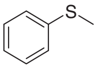	0.17	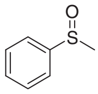 (98)	97
3	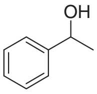	24	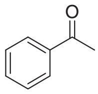 (99)	89
4	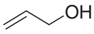	72	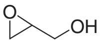 (50)	65
			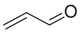 (23)	
			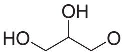 (27)	

[a]Reaction conditions: TBA_5**I** (4 µmol), substrate (1.0 mmol), 30% H_2O_2 (0.1 mmol), $HClO_4$ (2 equiv with respect to TBA_5**I**), CH_3CN (3 mL), 283 K. Yield and selectivity were determined by GC or ^{1}H NMR analysis. Yield (%) = total products (mol)/initial H_2O_2 (mol) × 100. Selectivity (%) = desired product (mol)/total products (mol) × 100.

gave the corresponding sulfoxide in 95% yield. In this case, the corresponding sulfone was hardly produced. 1-Phenylethanol was also selectively oxidized to acetophenone in 89% yield. Allyl alcohol was oxidized to the corresponding epoxide (50% selectivity), aldehyde (23% selectivity), and triol (27% selectivity). This selectivity for the TBA_5**I**-catalyzed oxidation of allyl alcohol is very different from those for triniobium-substituted-POM-catalyzed ones.[6] To the best of our knowledge, efficient H_2O_2-based oxidation by niobium-substituted POM catalysts applicable to various organic substrates is unprecedented.

In conclusion, a novel diniobium-substituted silicodecatungstate with two η^2-coordinated peroxo groups, $[\gamma\text{-HSiW}_{10}O_{38}Nb_2(\eta^2\text{-}O_2)_2]^{5-}$ (**I**) was successfully synthesized and characterized. The ^{29}Si and ^{183}W NMR, and CSI-MS spectra suggest that **I** reacts with H_2O_2 in the presence of protons to form the possible active species **II**. Compound **I** could efficiently catalyze the H_2O_2-based oxidation of various organic substrates in the presence of a suitable proton source.

Supporting Information is available electronically on J-STAGE.

References and Notes

† Present address: Materials and Structures Laboratory, Tokyo Institute of Technology, 4259 Nagatsuta-cho, Midori-ku, Yokohama, Kanagawa 226-8503

1 a) C. L. Hill, *Chem. Rev.* **1998**, *98*, 1. b) M. T. Pope, in *Comprehensive Coordination Chemistry II*, ed. by J. A. McCleverty, T. J. Meyer, Elsevier Pergamon, Amsterdam, **2003**, Vol. 4, pp. 635–678. doi:10.1016/B0-08-043748-6/03035-8. c) A. Proust, R. Thouvenot, P. Gouzerh, *Chem. Commun.* **2008**, 1837. d) D.-L. Long, R. Tsunashima, L. Cronin, *Angew. Chem., Int. Ed.* **2010**, *49*, 1736. e) L. Cronin, A. Müller, *Chem. Soc. Rev.* **2012**, *41*, 7333.

2 a) C. L. Hill, C. M. Prosser-McCartha, *Coord. Chem. Rev.* **1995**, *143*, 407. b) T. Okuhara, N. Mizuno, M. Misono, *Adv. Catal.* **1996**, *41*, 113. c) N. Mizuno, K. Yamaguchi, K. Kamata, *Coord. Chem. Rev.* **2005**, *249*, 1944. d) *Modern Heterogeneous Oxidation Catalysis: Design, Reactions and Characterization*, ed. by N. Mizuno, Wiley-VCH, Weinheim, **2009**. doi:10.1002/9783527627547. e) N. Mizuno, K. Kamata, *Coord. Chem. Rev.* **2011**, *255*, 2358. f) J.-Y. Piquemal, E. Briot, J.-M. Brégeault, *Dalton Trans.* **2013**, *42*, 29.

3 a) B. S. Lane, K. Burgess, *Chem. Rev.* **2003**, *103*, 2457. b) *Mechanisms in Homogeneous and Heterogeneous Epoxidation Catalysis*, ed. by S. T. Oyama, Elsevier, Amsterdam, **2008**.

4 a) Y. Goto, K. Kamata, K. Yamaguchi, K. Uehara, S. Hikichi, N. Mizuno, *Inorg. Chem.* **2006**, *45*, 2347. b) C. N. Kato, K. Hayashi, S. Negishi, K. Nomiya, *J. Mol. Catal. A: Chem.* **2007**, *262*, 25.

5 a) Y. Nakagawa, K. Kamata, M. Kotani, K. Yamaguchi, N. Mizuno, *Angew. Chem., Int. Ed.* **2005**, *44*, 5136. b) Y. Nakagawa, N. Mizuno, *Inorg. Chem.* **2007**, *46*, 1727. c) K. Kamata, K. Yonehara, Y. Nakagawa, K. Uehara, N. Mizuno, *Nat. Chem.* **2010**, *2*, 478. d) K. Yonehara, K. Kamata, K. Yamaguchi, N. Mizuno, *Chem. Commun.* **2011**, *47*, 1692. e) K. Kamata, K. Sugahara, K. Yonehara, R. Ishimoto, N. Mizuno, *Chem.—Eur. J.* **2011**, *17*, 7549. f) K. Kamata, T. Yamaura, N. Mizuno, *Angew. Chem., Int. Ed.* **2012**, *51*, 7275.

6 a) M. W. Droege, R. G. Finke, *J. Mol. Catal.* **1991**, *69*, 323. b) M. K. Harrup, G.-S. Kim, H. Zeng, R. P. Johnson, D. VanDerveer, C. L. Hill, *Inorg. Chem.* **1998**, *37*, 5550.

7 D. A. Judd, Q. Chen, C. F. Campana, C. L. Hill, *J. Am. Chem. Soc.* **1997**, *119*, 5461.

8 a) D. Bayot, B. Tinant, B. Mathieu, J.-P. Declercq, M. Devillers, *Eur. J. Inorg. Chem.* **2003**, 737. b) D. Bayot, B. Tinant, M. Devillers, *Catal. Today* **2003**, *78*, 439. c) S.-J. Li, S.-X. Liu, C.-C. Li, F.-J. Ma, D.-D. Liang, W. Zhang, R.-K. Tan, Y.-Y. Zhang, L. Xu, *Chem.—Eur. J.* **2010**, *16*, 13435. d) Q. Geng, Q. Liu, P. Ma, J. Wang, J. Niu, *Dalton Trans.* **2014**, *43*, 9843.

9 The ^{29}Si and ^{183}W NMR spectra of **I** were measured by using $TPeA_5$**I** because the solubilities of TMA_5**I** and TBA_5**I** in CD_3CN were below the detection limits of ^{29}Si and ^{183}W nuclei.

10 a) G. Wahl, D. Kleinhenz, A. Schorm, J. Sundermeyer, R. Stowasser, C. Rummey, G. Bringmann, C. Fickert, W. Kiefer, *Chem.—Eur. J.* **1999**, *5*, 3237. b) A. Hroch, G. Gemmecker, W. R. Thiel, *Eur. J. Inorg. Chem.* **2000**, 1107. c) D. V. Deubel, J. Sundermeyer, G. Frenking, *Org. Lett.* **2001**, *3*, 329. d) R. Ishimoto, K. Kamata, N. Mizuno, *Angew. Chem., Int. Ed.* **2012**, *51*, 4662.

11 Kinetic studies showed the first-order dependence of the reaction rates on the concentration of H_2O_2 (8.33–49.8 mM, Figure S7b). The dependence of the reaction rates on the concentration of **1** (0–1.33 M) showed saturation kinetics (Figure S7c) which can be explained by the change of the rate-determining step from the oxygen transfer step from **II** to the C=C double bond (at low concentration of **1**) to the regeneration of **II** with H_2O_2 (at high concentration of **1**) in a similar way to those of divanadium-substituted POMs.[5]